Received: 27 November 2019 | Revised: 20 February 2020 | Accepted: 20 March 2020

DOI: 10.1002/aic.16978

PROCESS SYSTEMS ENGINEERING

AIChE JOURNAL

Optimization of the amines-CO_2 capture process by a nonequilibrium rate-based modeling approach

Luis Angel López-Bautista | Antonio Flores-Tlacuahuac

Tecnologico de Monterrey, Escuela de Ingeniería y Ciencias, Monterrey, Mexico

Correspondence
Antonio Flores-Tlacuahuac, Tecnologico de Monterrey, Escuela de Ingeniería y Ciencias, Av. Eugenio Garza Sada 2501, Monterrey, N.L. 64849, Mexico.
Email: antonio.flores.t@tec.mx

Abstract

Amine-based chemical absorption has become the most mature technology among carbon dioxide capture processes, featuring the advantages of high separation efficiencies and its simplicity to attach it to existent industrial facilities. Nevertheless, further improvements on its performance are required in order to implement this technology to a wider extent. Energy expenditure at the solvent regeneration unit has been remarked as the major drawback of the process under discussion; therefore, the main objective of this work is to compute optimal operating policies which ensure minimum heat load at the reboiler along with reasonable removal efficiencies. A deterministic mathematical model of a reported pilot plant was deployed as the basis for the nonlinear programming optimization formulations, using a rate-based approach and an eNRTL thermodynamic framework. Several optimization scenarios were studied to account for diverse capture targets and degrees of freedom. Furthermore, sensitivity analyses were performed to understand the stand-alone effect of some variables on the process. Results reflect the importance of optimizing the complete plant to account for significant interactions between variables, as well as choosing an operational arrangement according to the separation goal demanded.

KEYWORDS

carbon dioxide capture, monoethanolamine, nonlinear programming

1 | INTRODUCTION

Climate change and environmental issues have been strongly linked to the generation and release of greenhouse gases into the atmosphere,[1] with Earth's temperature rise being remarked as the most immediate consequence of large concentration of such gases. Among all greenhouse gases, Carbon Dioxide has been mentioned as the main driver of this crisis.[2-4] This fact is not surprising if we consider the vast amounts in which CO_2 is produced anthropogenically: according to the US Environmental Protection Agency (EPA),[5] in 2017 roughly 82% of the greenhouse gas emissions coming from man-made sources were attributed to this gas. Moreover, that year power generation facilities contributed to approximately 33% of these CO_2 emissions whereas diverse industrial plants contributed with another 15% of such emissions; this is, nearly 50% of the discharges to the atmosphere were made by these major economic drivers.

In order to face this problem, renewable energy sources have emerged as alternatives for sustainable power generation; nevertheless, the development of these technologies is yet at early stages and the scientific community is still working on improving their efficiencies, as well as on deploying them at a scale which satisfies the increasing human energy demand. Along with this, the transition of established industries towards cleaner processes might take several years, that is why carbon dioxide capture processes (CCP) are considered to be a feasible solution to tackle this problem in the near future.[2,6]

Among all the CCP, chemical absorption employing amine solutions is the most mature and studied technology up to date,[7] featuring alkanolamines such as monoethanolamine (MEA), diethanolamine

(DEA), or N-methyldiethanolamine (MDEA) as recurrent solvents. Major advantages of this process include the high CO_2 removal efficiency that can be achieved (up to 90% or even greater), and the simplicity of attaching it to existent industrial and power plants. Plus, as a product of this process, high purity CO_2 is recovered and may be used as raw material in food industries or sent to storage at geologic wells. Nevertheless, this CCP presents several concerns which have stopped it from spreading faster around the world. First, amines are not environmental friendly solvents, thus leaks would represent risks for both nature and human beings' health. To address this issue, research and development regarding sustainable and efficient solvents must be encouraged, where full or partial replacement of amines with ionic liquids seems to be an optimistic path. Moreover, it has been widely reported that the main drawback of the amines-CO_2 process lays on its high energy consumption,[2,6,7] especially at the solvent regeneration unit; this fact certainly has a great impact on the economical point of view of the technology, and also from a sustainable perspective, hence making it less attractive for companies.

For dealing with the great energy demand of the system, in the present work we propose a deterministic nonlinear parameter optimization of a typical amines-CO_2 process, aiming to reduce the overall energy consumption while meeting CO_2 capture targets as well. To such purpose, we will deploy a rigorous first principles nonequilibrium and chemically reacting steady-state mathematical model of the given system. This nonequilibrium rate-based approach is adequate to capture all the phenomena that undergo the chemical species, and it is especially appropriate for complex systems like the one under discussion,[8,9] thus ensuring realistic results that may have a positive impact on the operating policies of these facilities.

The nonlinear programming (NLP) problems were solved in the GAMS optimization environment, different case studies were worked out to figure out the impact of main decision variables on the outputs, as well as to compare diverse scenarios which involve the optimization of a single equipment against the whole plant at different CO_2 capture goals. As previously stated, this work focuses on the optimization of operating parameters, hence some relevant decision variables include: feed rate of the solvent, operating pressures, temperature specifications, and reflux ratio. Furthermore, a main characteristic of this work is that we modeled the whole CCP, that is, considering both absorption and regeneration units, therefore the interaction between the equipment is taken into account yielding interesting results of the plant's complete scope.

2 | PROBLEM DEFINITION

Consider a flue gas stream which comes from a conventional thermal power plant, featuring typical composition, temperature and pressure for such a process,[2,6] as shown in Table 1, and assume that the CO_2 concentration should be reduced. To achieve this goal, the flue gas is fed into a CCP which performs chemical absorption using amine solutions, as displayed in Figure 1. As can be seen, the process is composed of two main units. In the absorption column, the flue gas stream is fed at the bottom, and it flows upwards inside the structure of the column interacting countercurrent with an amine solution which is fed at the top of the column. These interactions involve complex multicomponent mass transfer and chemical reactions that make possible the decrease of CO_2 in the gas stream. As products of the absorber, a treated clean gas stream (i.e., free or containing small amounts of CO_2) is obtained at the top of the column and released to the atmosphere, while in the bottoms stream a solvent, rich in CO_2 and products of the reacting system, leaves the absorption tower and is sent to a regeneration unit. A desorption–distillation column is the second main component of this process, its goal is to revert the reactions that took place in the absorber, thus obtaining as products a gaseous stream at the top containing CO_2 with high purity, and a liquid stream at the bottom containing a regenerated amine solution, which is then recirculated to the absorber. This stripper is equipped with a partial condenser and a reboiler, which provides the necessary heat to revert the reactions and, as mentioned above, is responsible of making this process energetically expensive. Furthermore, as observed in Figure 1, there is a heat exchanger between both columns which preheats the rich solvent that enters the stripper in an effort to reduce the heat duty of the reboiler, and a storage tank set just before the liquid feed to the absorber, which dampens any disruption on the concentration or temperature of the solvent that enters the process. There is also a solvent makeup stream to compensate for solvent lost through the process.

TABLE 1 Specifications for the flue gas stream fed into the absorber

Property	Value	Units
Flow rate	25.8845	kmol/hr
Temperature	324.14	K
Pressure	1	atm
Molar composition		
H_2O	0.0164	
CO_2	0.1618	
O_2	0.0484	
N_2	0.7734	

The CCP modeled in this work is based upon an existent pilot plant located at the University of Texas at Austin, which was used for the influential experimental report presented by Dugas.[10] Both absorber and stripper are similarly designed, with a height of 11.1 m each and an internal diameter of 0.427 m, built of carbon steel. They both have a pair of beds for packing with a height of 3.05 m each, this is, a single column may have a total packing height of 6.1 m. Regarding the internals, we chose the configuration of the last 24 runs from the experiments executed by Dugas,[10] i.e., the absorber is packed with IMPT no. 40, a well-known random metal packing, while the desorber is packed with Flexipac 1Y, one of the most widely used structured packing in the industry. Finally, the process is run using a solution of monoethanolamine as chemical solvent with a concentration of approximately 30 wt%, which is a common value for this system.[2]

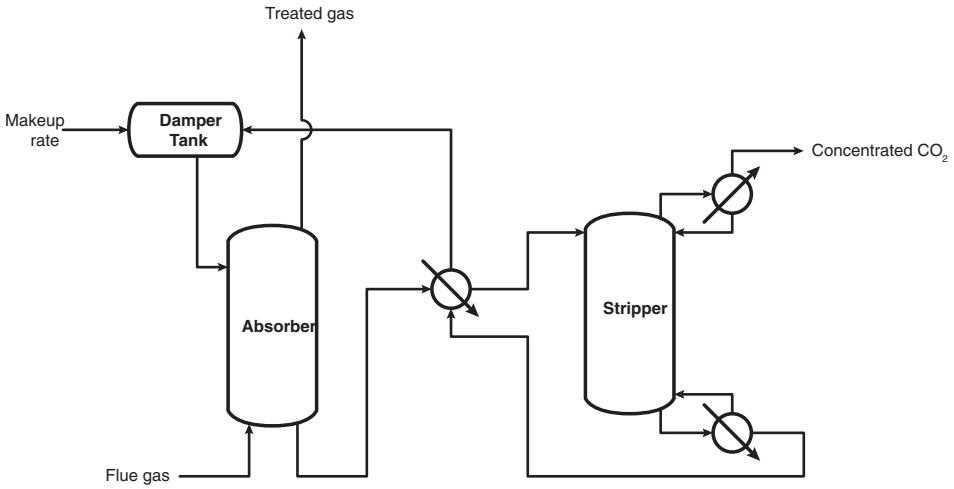

FIGURE 1 Diagram for the carbon dioxide capture process modeled in this work

As stated before, the main drawback of this technology is its high energy demand.[2,7] Hence, we present a deterministic gradient based nonlinear optimization approach aimed to find out optimal processing conditions featuring minimum energy consumption and meeting CO_2 capture efficiencies simultaneously. Up to our best knowledge, optimization studies with this degree of modeling complexity (i.e., rate-based models along with NLP) have not been reported in the open literature. Most of the research in the area concerns about the mathematical modeling of the process,[11-13] the phenomena involved within it,[14-17] or about process simulation employing software such as Aspen.[3,18,19] Some of these studies have performed sensitivity analyses on the process, for example, Chu et al.[20] modeled an industrial scale plant to study the responses of the columns to different operating pressures, heights, and packing materials, while Mac Dowell et al.[13] proposed a dynamic model of the process and performed sensitivity analyses varying the inlet lean solvent and inlet gas stream specifications. Regarding deterministic optimization, Mores et al.[21,22] performed a series of NLP problems on pilot plants, using a rate-based model but considering thermal equilibrium, and assuming ideal behavior in both phases; moreover, they did not account for a direct interaction between both columns. As can be seen, the problem is challenging and timely due to global warming concerns.

3 | PROBLEM FORMULATION

Ever since a long time ago, the limitations of physical equilibrium stage modeling of separation processes have been recognized,[8] especially when dealing with multicomponent systems and, even more, with reactive systems.[23] Traditionally, this approach suggests that both interacting phases are in thermodynamic equilibrium considering that sufficient stage contact time is allowed, yet it is common practice to assume that there exists mechanical and thermal equilibrium in each stage.[24] These conditions are unlikely to be found in practice, and normally the model is corrected by a stage efficiency term.

A more proper and rigorous approach when dealing with complex systems is based on deploying nonequilibrium stage or rate-based separation models. In this separation modeling approach, no assumption regarding thermodynamic or thermal equilibrium between the involved phases is made, rather it deepens on the mechanisms of mass and energy transfer which make the separation possible and which determine the temperature of the phases in a given stage. This is a more sophisticated model than its equilibrium counterpart, since it is able to capture most of the phenomena taking part inside the core of the separation equipment, making it more suitable to model systems as the one studied in this work.

The nonequilibrium model deployed in this research is based on the one proposed by Taylor and co-workers,[8] using Onda's and Bravo's correlations to compute mass transfer coefficients,[25,26] and the Chilton–Colburn analogy along with a penetration model to compute heat transfer coefficients.[9] Moreover, the electrolyte NRTL (eNRTL) model was employed as thermodynamic framework to account for nonidealities in the reacting liquid phase, whereas the vapor phase was assumed to behave as an ideal gas. The aforementioned thermodynamic framework considers a set of equilibrium reactions which take place on the liquid bulk, while an enhancement factor approach was used to represent the kinetic reactions occurring at the liquid side interphase. Due to space limitations, and in order to keep the content of this section straightforward, details of the complete model are presented in the Supporting Information section.

Our mathematical model was implemented in the GAMS Studio optimization environment (version 0.9.2), using the solver CONOPT 4 (version 4.06), an active-set reduced gradient algorithm designed for large scale nonlinear programming. The complete plant model as depicted in Figure 1 consists of approximately 32,800 variables and constraints when running the program as a process simulator, that is, with zero degrees of freedom, as it is the case for the results shown as model validation. Of course, when dealing with the optimization studies some variables will be released to have positive degrees of freedom. Typical solution times of the program are of a few minutes when giving the solver a good initial point; to do so, we built several programs adding one stage at a time, taking the values of the variables from the last stage modeled as initial points for the subsequent stage, until completing the total stages for each column. If a good initial

point is not given to the complete plant model, convergence is not ensured or the solver may take several hours to reach feasibility. The GAMS codes employed to generate some of the results presented in this work are available at: http://github.com/antonio-flores-tlacuahuac/publications/2020/Amines-CO2capture.

The case to be reproduced in this research as model validation corresponds to run number 29 of the pilot plant, where a solution of 30% mass is fed to the absorber according to the conditions presented in Table 2. This case will be referred to as the base case for our work; it was chosen that way because it represents an instance where the absorber operates at a medium value of the gas to liquid ratio (as classified by Zhang et al.[18]), and thus it will give us the flexibility to move upwards and downwards to other operating regimes.

It is important to mention that the process was also simulated in Aspen Plus using for both columns the built-in rate-based separation model "RadFrac"; this was done in order to compare the profiles obtained by such a high level simulator against our mathematical model. Now, let us start discussing the validation results for the absorber. Some of the main assumptions made on the mathematical description of this column are that it is considered as an adiabatic equipment, the pressure drop on the column internals are negligible, it operates at atmospheric pressure, and the bulk phases are modeled as perfectly mixed, this means that the properties of the each bulk are equal to the properties leaving the stage for its corresponding phase. The profile for the removal of CO_2 on the vapor phase is shown in Figure 2, while the liquid bulk temperature profile is depicted in Figure 3. Notice that the stages on the columns were numbered from the top bottom, that is, the Stage 20 corresponds to the bottom of the column while Stage 1 is the upper stage.

As can be seen from Figure 2, the composition profiles of CO_2 obtained by our mathematical model and by the Aspen Plus simulation are in excellent agreement, showing an overall deviation of only 3.06% from one another. From such a plot, it is observed that CO_2 concentration in the vapor phase diminishes as the fluid moves upwards in the column, meeting with the chemical solvent. The separation rate is faster in the bottom stages, deploying a quasi-linear behavior until Stage 10; afterwards, a slight curvature is observed and the separation rate of CO_2 in the upper stages becomes minimal. According to experimental data, the molar CO_2 composition of the gas leaving the absorber on top of the column in run 29 is 0.0532,[3] while our mathematical model predicted a molar composition of 0.0462 for the same effluent, this is, there is an absolute deviation of 13.11%. Moreover, an experimental CO_2 removal percent of 70% was reported for this case,[18] where our model predicted a removal percent of 70.5%, i.e., there is only 0.71% of deviation on this critical parameter.

Furthermore, from Figure 3, it is observed that the liquid temperature profiles of the absorber predicted by our model and obtained from Aspen Plus are also in good agreement. This is a commonly studied profile in chemical absorption since it reflects the reactions taking place in the column internals. In spite of the fact that our model slightly overestimates the temperatures of the stages behind the

TABLE 2 Specifications for the amine solvent fed into the absorber, base case

Property	Value	Units
Flow rate	140.4958	kmol/hr
Temperature	313.15	K
Pressure	1	atm
Molar composition		
H_2O	0.8457	
MEA	0.1201	
CO_2	0.0342	

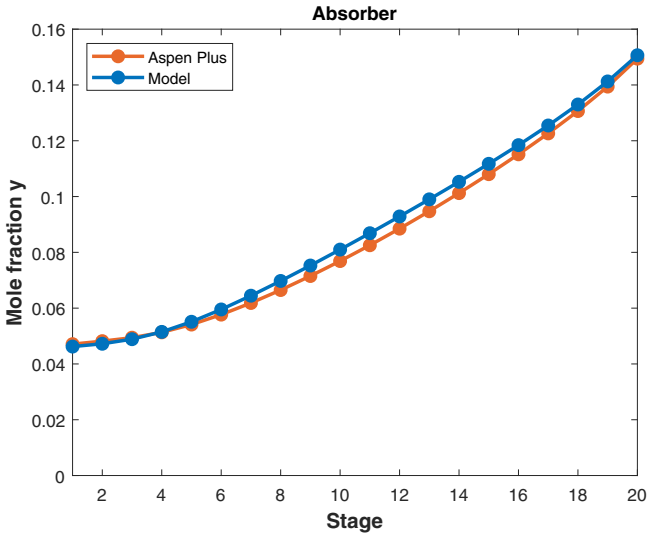

FIGURE 2 Molar composition profile of CO_2 in the absorber, base case [Color figure can be viewed at wileyonlinelibrary.com]

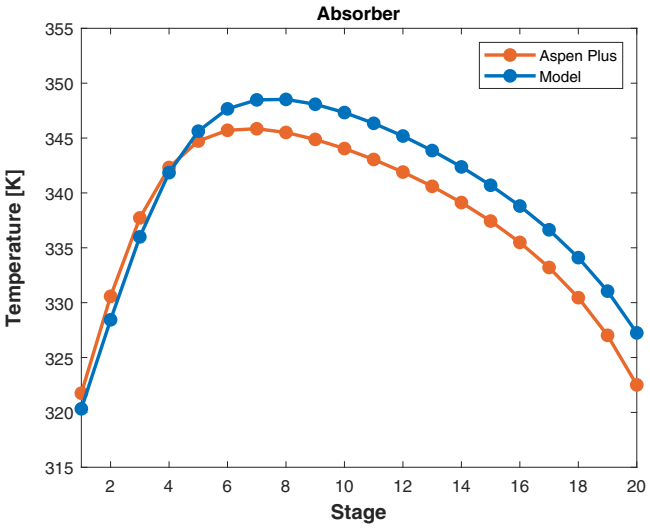

FIGURE 3 Liquid phase temperature profile in the absorber, base case [Color figure can be viewed at wileyonlinelibrary.com]

inflection point, the overall discrepancy between both data is of only 0.84%. More important is to notice that our model is able to capture the bulge on the curve, which is typical for this specific process. Moreover, this case has a medium L/G ratio as mentioned before, so it is expected that the temperature drops abruptly at both edges of the column,[18] such trend is also well captured in our model.

For further discussion on the stripper validation, as well as on the thermodynamic method validation, the reader is referred to the Supporting Information section.

4 | OPTIMIZATION FORMULATION

Once the amines-CO_2 reaction-separation mathematical model has been validated, several optimization scenarios which yield optimal operating conditions of the addressed system are proposed. The deterministic nonlinear programming (NLP) problem is formulated as follows:

$$\min_{\mathbf{x}} \ \Omega = \mathbf{F}(\mathbf{x}) \tag{1}$$

$$\text{Subject to}: \quad \mathbf{h}(\mathbf{x}) = 0 \tag{2}$$

$$\mathbf{g}(\mathbf{x}) \le 0 \tag{3}$$

$$\mathbf{x}^L \le \mathbf{x} \le \mathbf{x}^U \tag{4}$$

where Ω is the objective function, $\mathbf{F}$ is the particular form of the objective function, and $\mathbf{x}$ is a vector of decision variables. Moreover, $\mathbf{h}$ represents a vector of equality constraints, including mass and energy balances, the thermodynamic method, and further correlations described in the Supporting Information section, whereas $\mathbf{g}$ stands for a vector of inequality constraints, which might include operating limits and minimum CO_2 capture targets. Finally, superscripts L and U denote lower and upper bounds, respectively; these are commonly imposed by physical restrictions.

In order to explore diverse features of the process being discussed, we depicted three different objective functions which are defined as follows:

Omega A:

$$\max_{\mathbf{x}} \Omega_A = \boldsymbol{\alpha} \tag{5}$$

where $\boldsymbol{\alpha}$ denotes the CO_2 removal percent. This objective function aims to find the operating conditions which boost the gas sequestration at the absorption column. We argue that measuring the efficiency of the separation in terms of the removal percent is a better approach than doing it by minimizing the CO_2 mole fraction of the gas exiting at the top of the column, since $\boldsymbol{\alpha}$ takes into account both flow rate and mole fraction, and interferences from dilution or mass transfer through the interphase of other species may be avoided.

Omega B:

$$\min_{\mathbf{x}} \Omega_B = \mathbf{Q}_{reb} \tag{6}$$

This objective function embodies the main motivation behind this work, and aims to obtain a set of operating conditions which minimizes the heat duty of the stripper reboiler, $\mathbf{Q}_{reb}$. As will be detailed in the upcoming section, this objective function is used in conjunction with additional restrictions to account for separation goals.

Omega C:

$$\min_{\mathbf{x}} \Omega_C = \frac{\mathbf{Q}_{reb}}{\text{kmol of } CO_2 \text{ recovered}} \tag{7}$$

This last objective function has an interesting meaning if we examine it from its units perspective: kJ/kmol. It aims to minimize the amount of energy added into the system needed to remove a unit of CO_2 fed into the process. As with its Ω_B counterpart, this function is usually deployed along with separation target constraints.

5 | RESULTS AND DISCUSSION

The results of a series of studies performed in this work are presented and analyzed below, aiming to identify operating conditions which bear to minimum energy demand considering separation efficiency as well. This section is divided into two major subsections: sensitivity analyses and optimization scenarios. In the former, a set of sensitivity analyses were carried out for some of the absorber key variables (i.e., L/G ratio, operating pressure, and feed temperature of the solvent), while keeping all the other parameters fixed as in the base case (Tables 1 and 2); this was done in order to study and understand the impact that such variables would have on the overall process output, as well as for establishing comprehensible operating bounds on decision variables. It should be noticed that the interaction between these variables in the upcoming optimization scenarios may be relevant and even counterintuitive, nevertheless we consider that these sensitivity analyses represent a good first approach in perceiving the system behavior. Moreover, in the optimization scenarios we study the objective functions described in the previous section. We deployed such functions for three different capture goals: (a) Unrestricted removal targets, (b) CO_2 removal target ≥70.5% (i.e., same separation efficiency as the base case), and (c) CO_2 removal target ≥90%. Furthermore, these scenarios were evaluated having decision variables released only in the absorption column and also with decision variables released in the whole process. Further details on the optimization studies are given at the beginning of the correspondent subsection. Finally, the benefits and drawbacks of each case were compared based on the mole fraction of CO_2 in the gas leaving the absorber, the CO_2 removal percent, and the energy loads in both reboiler and condenser.

5.1 | Sensitivity analyses

5.1.1 | Effect of L/G ratio on the process

First, we study the influence of the liquid to gas flow rate ratio (L/G ratio) fed into the absorber on some of the most important system outputs. To do so, we will vary the value of the liquid solvent flow rate entering the column, while keeping its temperature and composition fixed; the flow rate, temperature and composition of the vapor to be treated is fixed as well. We decided to move the L/G ratio in accordance with the classification given by Zhang et al.[18] for this process, starting from a low value (L/G approximately equal to 3.7), passing through a medium value (L/G approximately equal to 5.2), and ending with a high value (L/G approximately equal to 6.9). Figure 4 shows the temperature profiles for each of these cases; such profiles are important since they provide an indirect glance at the processes taking place inside the equipment, especially those related to mass transfer and reaction rates. It should be noticed that depending on the value of the L/G ratio we can change the position of the so-called temperature bulge. From Figure 4a it can be seen that when the operation involves a low L/G ratio such a bulge occurs at the top of the column, with an abrupt temperature decrease towards the bottom of the absorber, whereas from Figure 4c it can be observed that the bulge settles completely at the bottom of the column, with the temperature decreasing towards the upper stages. Figure 4b may be interpreted as a transition between both curves, with the bulge wide open through most of the stages, and a sudden temperature drop at both edges. It is also interesting to see that as the value of the L/G ratio increases, the number of stages in which $T^L > T^V$ decreases, this fact can only be noticed using rate-based models.

As aforementioned, the temperature profiles of the absorber are well studied and important curves, and all the CO_2 capture columns' behaviors may be included in one of the three classifications discussed above depending on their operating conditions, regardless of the scale and internals of the column (see, e.g., Zhang et al.,[18] Kale et al.,[12] Mores et al.,[21] and Mac Dowell et al.[13]).

Furthermore, in Figure 5 some relevant outputs of the process are depicted. As expected, we see from Figure 5a that increasing the L/G ratio has a positive impact on the separation efficiency; in fact this impact is quite significant since it may rise the CO_2 removal from a poor 57% up to an attractive 79% in the given conditions. Moreover, it is interesting to observe the behavior of this variable on the stripper

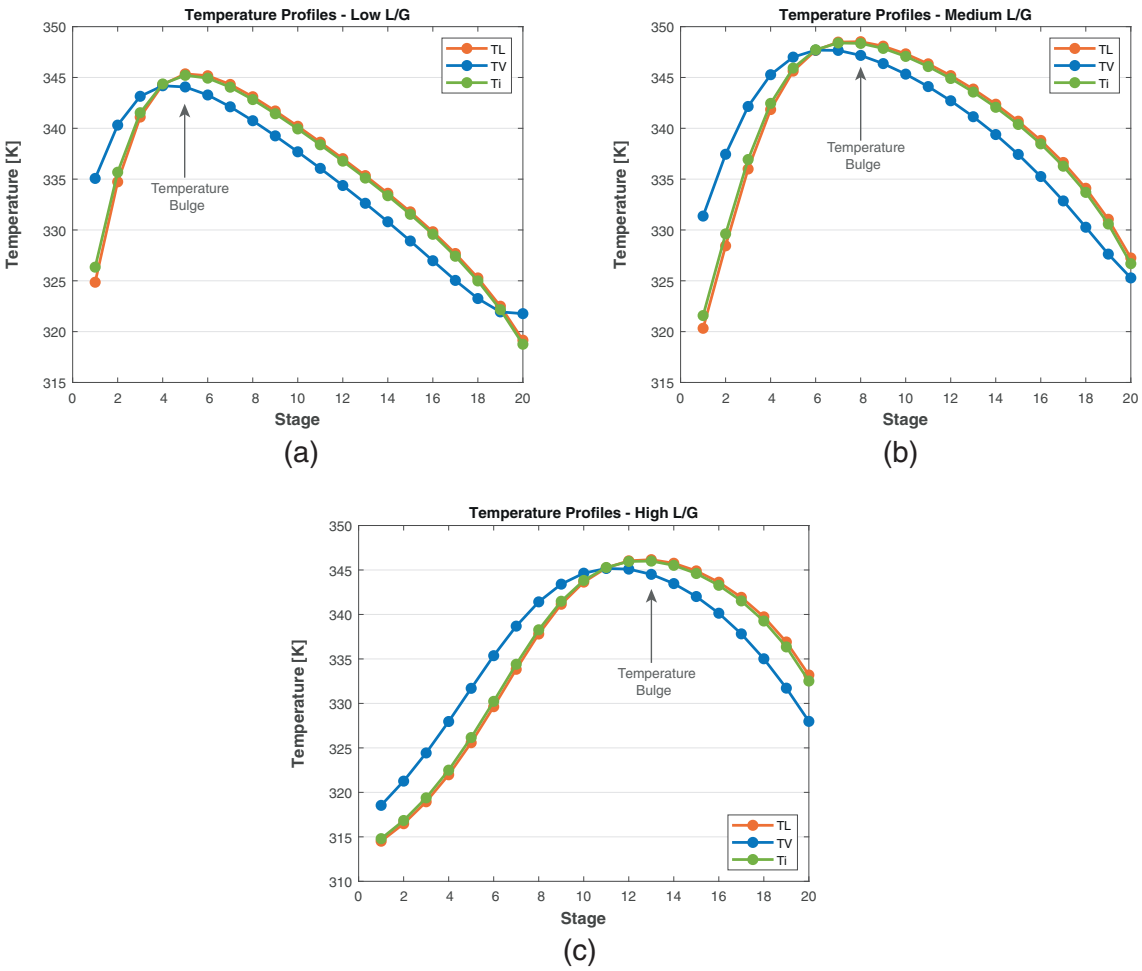

FIGURE 4 L/G ratio effect on the absorber temperature profiles: (a) Low L/G ratio; (b) Medium L/G ratio; (c) High L/G ratio [Color figure can be viewed at wileyonlinelibrary.com]

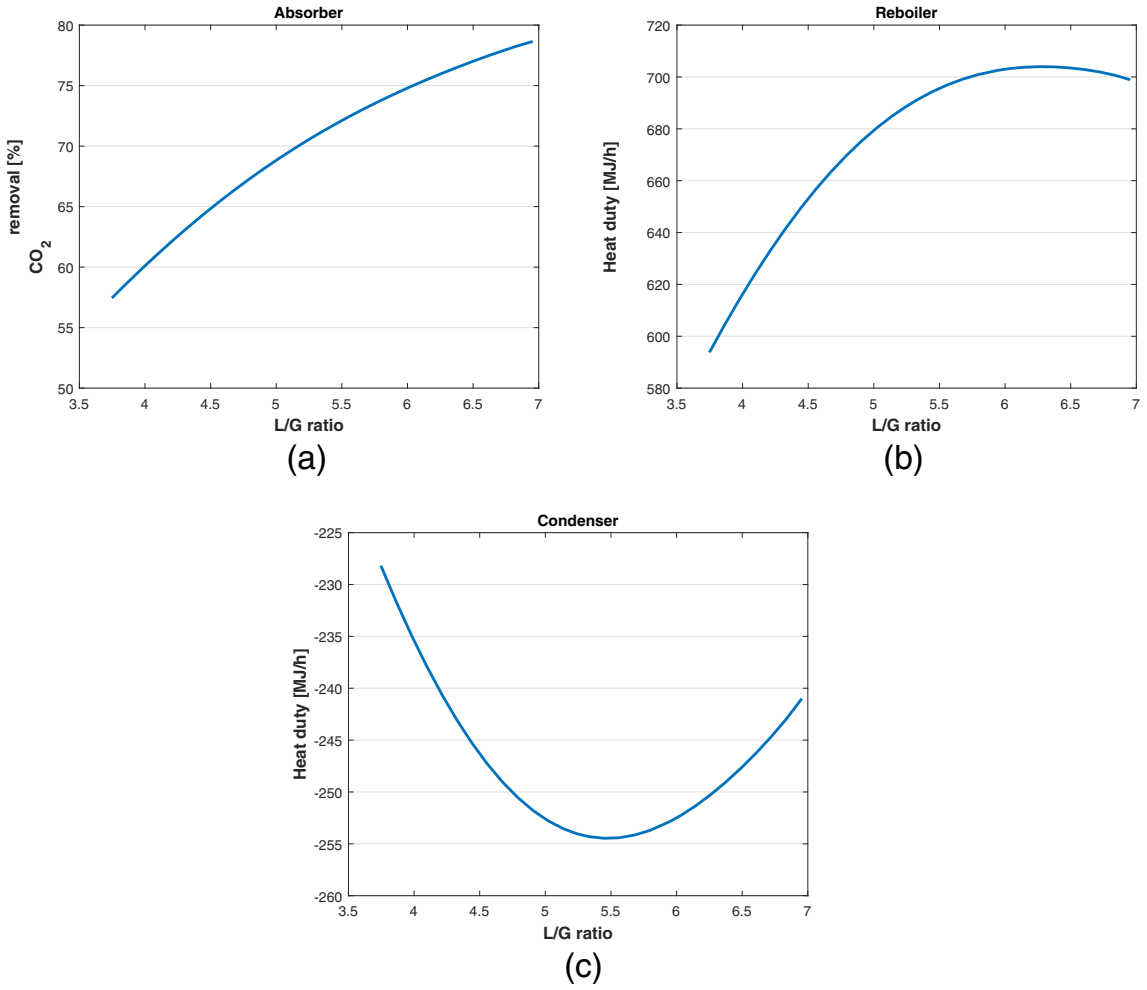

FIGURE 5 L/G ratio effect on some system's outputs: (a) CO_2 removal percent at the absorber; (b) Reboiler's heat duty at the stripper; (c) Condenser's heat duty at the stripper [Color figure can be viewed at wileyonlinelibrary.com]

reboiler and condenser, as shown in Figure 5b,c. We can see that in both curves there is an inflection point which represents the maximum energy that each equipment needs for operating, this point appears at an approximate value of L/G equal to 6.2 for the reboiler and L/G equal to 5.4 for the condenser. From such figures we would recommend to operate the process at L/G values which overcome the inflection point, that is, high L/G ratios, since we would obtain a better separation featuring less energy demand than operating at medium L/G ratios which are located just before the inflection point.

5.1.2 | Effect of the absorber operating pressure on the process

A second sensitivity analysis was performed to study the influence of the absorber operating pressure on some key outputs of the system. Such pressure was varied in a range starting from 0.5 until 5 atm in an effort to cover both low and moderately high pressure values, keeping in mind that our model assumes ideal behavior on the gas phase (larger pressure values would deviate from this assumption). The results obtained for this study are shown in Figure 6. It can be seen from Figure 6a that the efficiency of the separation decreases drastically below atmospheric pressure. Nevertheless, the efficiency rises for values above 1 atm, albeit in a slow fashion. In fact, the enhance in separation when operating at high pressures is not as significant as the behavior observed in the previous study: it rises from 70% at 1 atm to 83% at 5 atm. Similar trends to the curve on Figure 6a were observed by Chu et al.[20] when performing a parametric study on an industrial scale plant. They suggested to operate the column at atmospheric pressure.

Regarding energy requirements of the process, it is interesting to notice that the behavior of the separation efficiency curve in Figure 6a is similar to both the heat needed at the reboiler in Figure 6b and the condenser requirements in Figure 6c. The latter curve is rotated upside down due to the sign, which reflects that energy is removed from the system. Both Figure 6b,c suggest that low energy demands are required for operating pressures at the absorber around the atmospheric value.

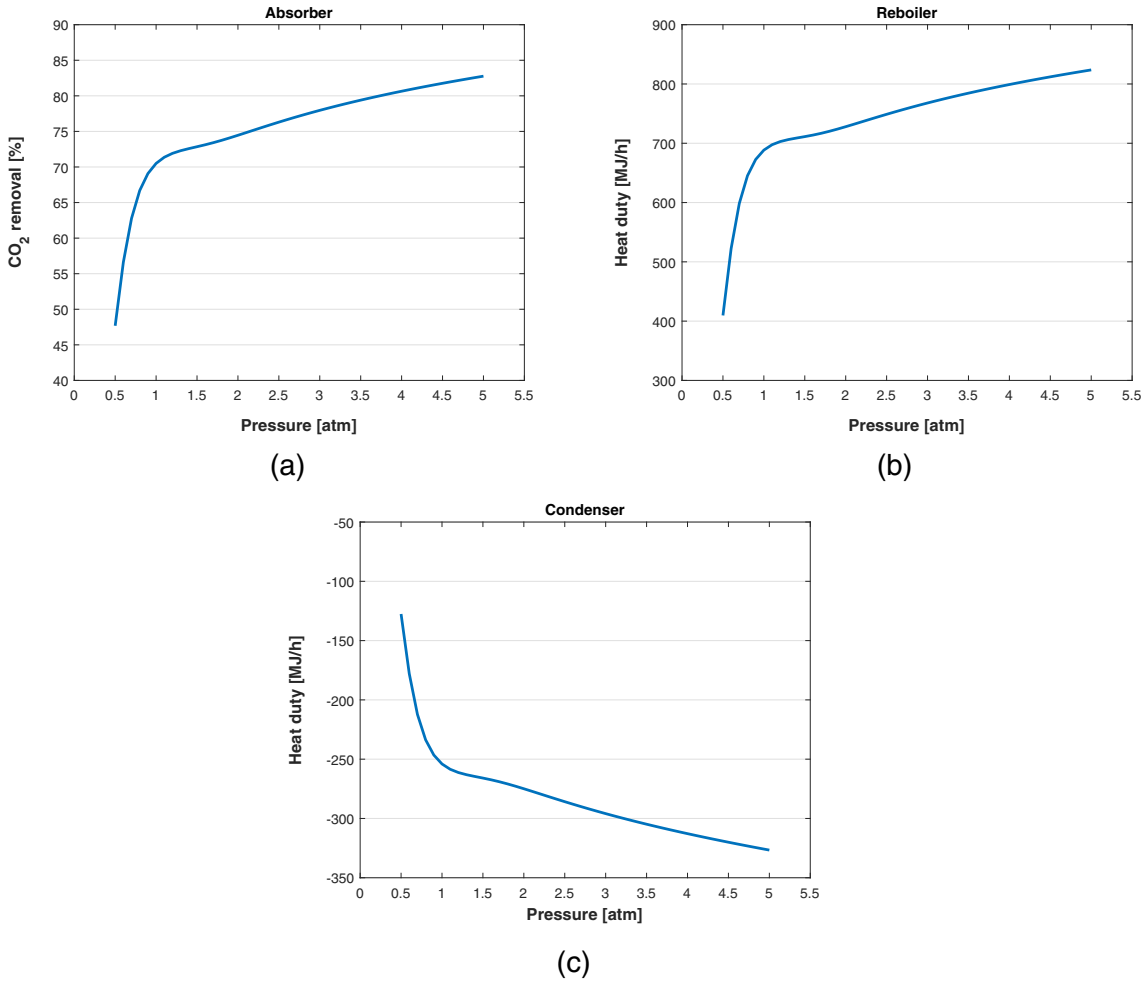

FIGURE 6 Absorber operating pressure effect on some system's outputs: (a) CO_2 removal percent at the absorber; (b) Reboiler heat duty at the stripper; (c) Condenser's heat duty at the stripper [Color figure can be viewed at wileyonlinelibrary.com]

5.1.3 | Effect of the liquid solvent feed temperature on the process

Below we discuss the effect of feeding the amine solution to the absorption column at different temperatures. We will vary such temperature from 300 to 353.15 K, the latter being a temperature far enough from the normal boiling point of water, as well as from the amine degradation temperature. The results for this sensitivity analysis are depicted in Figure 7. It can be seen from Figure 7a that there is a modest decrease in the CO_2 mole fraction of the gas leaving the absorber as the feed temperature of the solvent rises. Nevertheless, it is important to observe from Figure 7b that the separation efficiency is kept at a practically constant value of 70% ± 1% throughout the whole temperature range. In fact, for temperatures higher than 315 K it is observed that the efficiency slightly diminishes when increasing the temperature; this behavior occurs because even though the component mole fraction decreases, the total vapor flow rate rises. That is why we emphasize that separation processes like the one at hand should be analyzed considering not only the species concentration, but also the removal efficiency. Moreover, it can be noted from Figure 7c,d that more energy is required from the system when operating with solvents at higher temperatures, although in general it does not have a large impact since, looking at the scale of the *y* axis of Figure 7c, the energy at the reboiler fluctuates from approximately 675 to 694 MJ/hr. These ideas agree with Abu-Zahra et al.,[19] who modeled a large scale commercial plant and suggested that the lean liquid solvent should be fed at low to moderate temperatures.

5.2 | Optimization scenarios

In this subsection, we will discuss the results obtained from a series of optimization scenarios deployed in this work. As previously stated, these optimization studies were classified into three major groups, which we will refer to as *cases*. In Case 1 we performed optimization scenarios with unrestricted removal targets, this was done in order to know the limits or extents that the process may present without taking into account the removal efficiency. For this case, the objective functions Ω_A, Ω_B, and Ω_C were investigated. Furthermore, in Case 2 we conducted optimization scenarios where the CO_2 removal

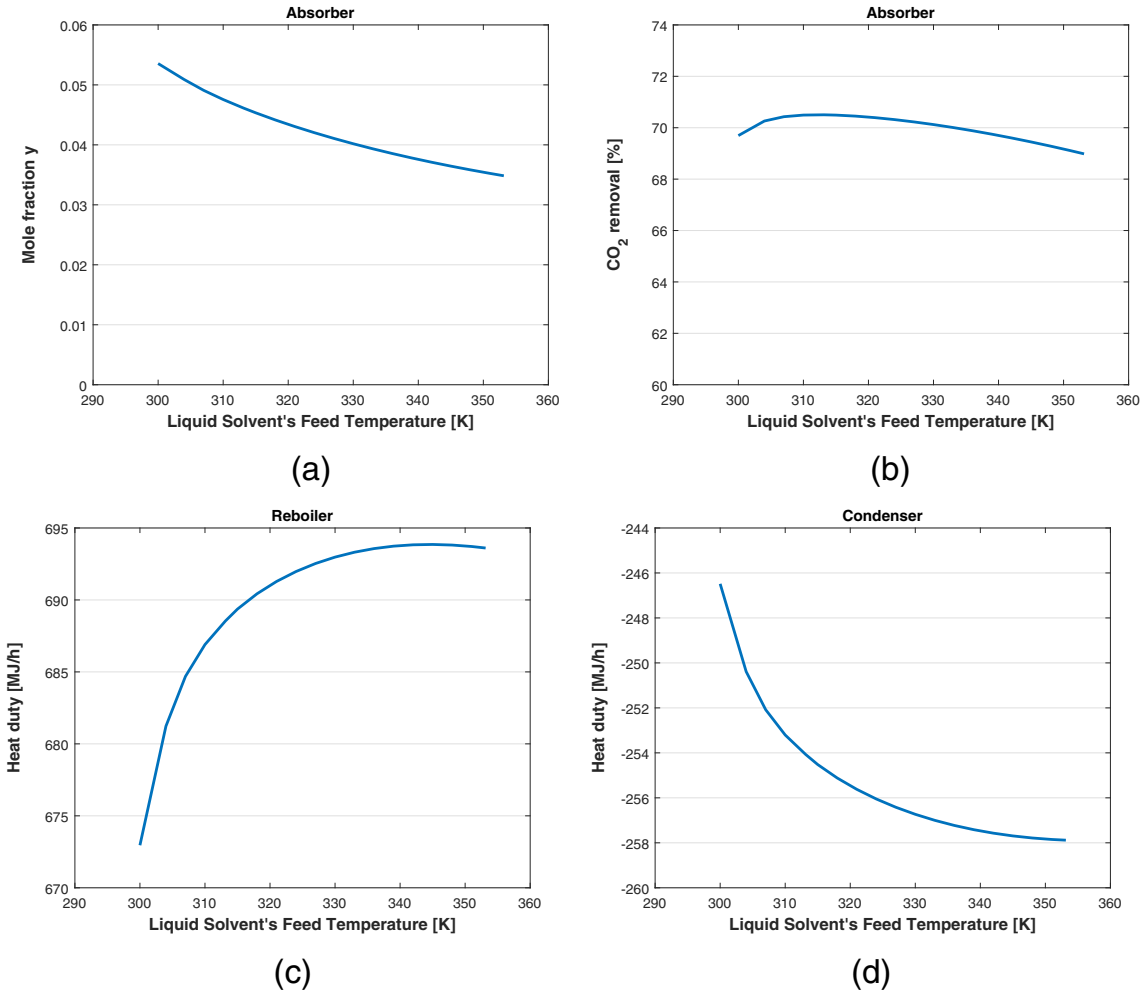

FIGURE 7 Liquid solvent feed temperature effect on some system outputs: (a) CO_2 mole fraction of the gas exiting the absorber; (b) CO_2 removal percent at the absorber; (c) Reboiler heat duty at the stripper; (d) Condenser heat duty at the stripper [Color figure can be viewed at wileyonlinelibrary.com]

efficiency was set to be ≥70.5%. Since this value is the same as the base case (as mentioned in Section 3), we can draw comparisons regarding the amount of energy consumption reduced via advanced numerical optimization techniques. For this case, we only investigated the objective functions Ω_B and Ω_C. Finally, in Case 3 the optimization scenarios involved a CO_2 removal efficiency ≥90%. This case was proposed since, according to the US Department of Energy (DOE),[7] such percentage represents a reasonable capture goal when implementing this technology in industrial plants and power generation facilities. As done for the second case, in the last one we only evaluated the objective functions Ω_B and Ω_C.

Moreover, for each of the aforementioned cases, two different situations were studied regarding the degrees of freedom: having variables released only at the absorption column and having variables released in the whole process. The variables released at the absorber are those described in the sensitivity analyses, using the same bounds; therefore, these scenarios would have up to three degrees of freedom. On the other hand, the situation which has variables released all over the process involves those three variables in the absorber plus other three variables released elsewhere: the temperature output specification of the heat exchanger located at the middle of the columns (with bounds set at 300 and 354 K), the reflux ratio of the stripper (with bounds set at 1.2 and 5 in mole basis), and the operating pressure of the stripper (with bounds set at 0.5 atm and 5 atm); this means that these situations may have up to six degrees of freedom. The above discussion is synthesized in Table 3. Furthermore, it should be mentioned that, for all the studies involving six degrees of freedom, an additional constraint was imposed demanding that the mole fraction of CO_2 in the vapor leaving the stripper be ≥0.93, thus ensuring a high concentration of such a species in the column's distillate.

The results for all the optimization scenarios are shown in Table 4. Subsequently, a brief discussion is given for each case. Finally, overall remarks are provided in Section 5.2.4.

5.2.1 | Case 1: Unrestricted removal targets

As aforementioned, the scenarios of this case let us explore the boundaries of the system. Case 1 Scenario 1 was the only instance

TABLE 3 Variables released for degrees of freedom

Variable description	Lower bound	Upper bound
Situations with 3 degrees of freedom		
Liquid solvent feed rate[a]	97 kmol/hr	180 kmol/hr
Absorber's operating pressure	0.5 atm	5 atm
Liquid solvent feed temperature	300 K	353.15 K
Situations with 6 degrees of freedom[b]		
Stripper's reflux	1.2	5
Stripper's operating pressure	0.5 atm	5 atm
Heat exchanger temperature specification	300 K	354 K

[a]To modify L/G ratio.
[b]Variables in addition to the ones of the previous situations.

were the objective function Ω_A was studied, releasing only variables on the absorber, since substantially such variables are the ones which have influence on the CO_2 removal efficiency. From the results shown in Table 4, it is clear that we may obtain a separation efficiency up to 99.45%, but as a trade-off the process runs with a high energy expenditure (in fact, the highest among all the experiments carried out in the present work). The operating conditions dictate that for reaching such a separation degree, the column must run with both high L/G ratio and high pressure, along with a moderate temperature of the solvent. We may conclude that, in spite of the fact that the process may reach to remove practically all the CO_2 from the flue gas to be treated, such an efficiency is excessive and, for technical and economical purposes, nonviable. Therefore, it is convenient to set comprehensible capture goals featuring low energy requirements.

Furthermore, in the subsequent scenarios of Case 1, the objective functions Ω_B and Ω_C were deployed aiming to find conditions to operate with minimum energy. It can be noted that Scenarios 2 and 3 suggest a similar arrangement in the optimized variables, differing only in approximately 14 kmol/hr of the solvent fed. Both scenarios agree that, when the stripper set up is fixed as in the base case, the minimum energy is obtained by running the absorber at low pressure and low temperature of the solvent, but a medium L/G ratio. Moreover, Scenarios 4 and 5 look for the minimum energy using all the degrees of freedom available in this work. In said scenarios, the interaction between variables recommend that the absorber should work at low L/G ratio and low pressure, but a moderate temperature of the solvent, while the stripper should be operated with both low reflux and pressure. It is evident that Scenarios 4 and 5 (i.e., the optimization studies with more degrees of freedom) lead to lower energy requirements, but also to better efficiencies of separation than Scenarios 2 and 3.

Even though Scenarios 2–5 have low energy demands, their CO_2 removal is really poor (efficiencies of 52% at best), that is why this optimization studies must be performed along with additional restrictions to account for separation targets. Finally, concerning the boundaries of the system, the lowest reboiler energy requirement was obtained in Scenario 4, being 113 MJ/hr, while the lowest capture efficiency among all the experiments was observed in Scenario 2, with a value of 35%.

5.2.2 | Case 2: CO_2 removal target ≥70.5%

The main purpose of this case is to establish a point of comparison against the base case in terms of CO_2 capture. The objective functions Ω_B and Ω_C were studied in this set of optimization scenarios, where both objective functions yielded the same output for each of the situations (i.e., when releasing variables only at the absorber and through the whole process), that is why the results of this case are presented only in two rows of Table 4. It is interesting to observe the differences in the absorber arrangement depending if the optimization was carried out only on such a column variables or if the optimization involved both column variables. In the former situation, it is suggested to run the absorption column at high L/G ratio, whereas in the latter, a more subtle medium L/G ratio is recommended.

One of the main outcomes of the situation at issue is the enhancement in energy demand on each scenario. When optimizing only the absorption column, although there is a decrease in the reboiler heat duty, this is of only 13% with respect to the base case. On the other hand, when the optimization takes into account both columns, an attractive saving of up to 68% can be achieved. Moreover, the results of Ω_C indicate that in Case 2 Scenario 1 an amount of 4.68 MJ must be supplied at the reboiler per each kg of CO_2 recovered at the absorber, while for Case 2 Scenario 2 we would only need to employ 1.72 MJ per kg of CO_2 captured. This case is a clear indicator of the importance of considering the whole process when aiming to optimize this kind of technology.

5.2.3 | Case 3: CO_2 removal target ≥90%

This case constitutes the most complete study among the optimization problems proposed in the present work, since it involves competitive separation efficiency while taking care of the energy requirements of the system. Just like the previous case, the objective functions Ω_B and Ω_C conducted to the same output for each of the situations related to the degrees of freedom, therefore the results for this case are also presented only in two scenarios. It can be noted that in this case the model recommends a similar configuration of the absorber for both scenarios: operating at high L/G ratio while slightly raising the column pressure in order to achieve the separation degree demanded. The main difference between the operating conditions of both scenarios lays on the stripper arrangement, with Scenario 2 suggesting an interaction of low reflux and low pressure for such a column. Furthermore, the outcomes of deploying the objective function Ω_C show that, in Case 3 Scenario 1, the reboiler requests 5.13 MJ of energy per kg of CO_2 captured in the first column, whereas in Case 3 Scenario 2 a reasonable amount of 2.97 MJ of energy are required by the reboiler per kg of CO_2 captured at the absorber. Besides the

TABLE 4 Results of the optimization scenarios

			Optimized variables						Process' output			
Scenario	Objective function	Degrees of freedom	Liquid feed rate (kmol/hr)	Pressure absorber (atm)	Temp. Solvent (K)	Heat exchanger spec. (K)	Reflux	Pressure stripper (atm)	y_{CO_2} leaving absorber	CO_2 removal (%)	Q_{Reb} (MJ/hr)	Q_{Cond} (MJ/hr)
Base case												
–	–	–	135.69	1	313.15	354	2	0.6804	0.04612	70.5	696.13	−255.02
Case 1: Unrestricted removal targets												
1	Ω_A	Absorber	180	5	321.46	354[a]	2[a]	0.6804[a]	0.00107	99.45	978.14	−371.64
2	Ω_B	Absorber	161.20	0.5	298.15	354[a]	2[a]	0.6804[a]	0.10604	35.40	276.80	−55.13
3	Ω_C	Absorber	147.90	0.5	298.15	354[a]	2[a]	0.6804[a]	0.10243	37.63	286.54	−66.18
4	Ω_B	Process	97	0.5570	327.02	354	1.2	0.6578	0.06811	47.41	113.09	−28.57
5	Ω_C	Process	97	0.6391	307.98	354	1.2	0.6387	0.07116	51.46	116.68	−33.93
Case 2: CO_2 removal target ≥ 70.5%												
1	Ω_B, Ω_C	Absorber	180	0.8768	307.81	354[a]	2[a]	0.6804[a]	0.05160	70.5	608.80	−197.44
2	Ω_B, Ω_C	Process	143.03	0.8921	314.98	354	1.2	0.6722	0.04498	70.5	223.39	−53.44
Case 3: CO_2 removal target ≥ 90%												
1	Ω_B, Ω_C	Absorber	180	1.6832	313.68	354[a]	2[a]	0.6804[a]	0.01856	90	851.61	−307.10
2	Ω_B, Ω_C	Process	180	1.6874	314.46	354	1.2	0.6661	0.01852	90	492.79	−121.90

[a]Fixed as in base case.

fact that this case presents an attractive separation efficiency, it can be noted that Case 3 Scenario 2 runs using lower energy requirements than the base case (29% of saving).

5.2.4 | Summary of results

After performing all the optimization studies proposed in this work, it is convenient to analyze overall remarks from the results displayed in Table 4. It is evident that running the absorption column at medium to high L/G ratio values is preferred, along with low to moderately low operating pressures. Also, the model suggests that the liquid solvent be fed at moderate temperatures (less than 315 K for all cases).

An interesting outcome is that, for all the studies deployed, the highest temperature specification of the heat exchanger located at the middle of both columns is endorsed. It should be reminded that the purpose of such an exchanger is to pre-heat the liquid solution entering the stripper. Therefore, it can be concluded that this exchanger plays an important role in supporting the stripper reboiler with the energy load. Furthermore, according to our model, low reflux and low pressure of the stripper are always recommended.

As expected, better results are obtained when more released variables are involved within the optimization problem. These kind of deterministic approaches are always encouraged since they internally account for complex interactions between the decision variables. Finally, it is interesting to observe that, even though all rate-based models are somehow system specific since they take into account the physical specifications of the columns, the results presented in this research are flexible enough to be compared against other plants of different scales as we have discussed throughout Section 5.1. This suggests that our outcomes may be applicable to a wide scope of CO_2 capture columns, nevertheless, the authors encourage the idea that for better results a specific rate-based model should be deployed for each column's unique configuration.

6 | CONCLUSIONS

Chemical absorption using amine solutions is nowadays the most mature technology among the CCP. Nevertheless, it presents several drawbacks (especially regarding energy loads) that are yet to be addressed in order to further attach this process to a wider range of industrial facilities. This work has demonstrated the importance of implementing rigorous mathematical modeling and deterministic optimization as a key towards the enhancement of sustainable processes,[27] and also as a support for subsequent practical deployment.

Particularly for the process at hand, rate-based modeling along with the eNRTL thermodynamic method and proper mass and energy relations have shown to constitute an adequate focus to capture the principles of the system; therefore, they are a powerful tool for obtaining realistic outputs from the optimization scenarios. Results illustrate that optimizing the complete process yields larger energy saving than optimizing the equipment individually. This implies that interactions between variables are relevant and their behavior is not always intuitive. Moreover, it is crucial that, depending on each industry requirements, separation efficiencies be considered through additional constraints in order to perform an optimization study for minimizing energy while achieving such a capture goal. This is encouraged since it was shown that according to the separation efficiency demanded, the model optimization recommends diverse operating arrangements. By applying the optimal operating policies suggested by the model, a theoretical energy reduction of up to 68% was achieved compared against the base case experimental data. Nevertheless, more realistic industrial data indicate that the energy required by the reboiler in conventional amines-CO_2 processes is around 4 GJ/tonCO_2.[28] In our work, we found that this ratio could be reduced until 2.97 GJ/tonCO_2 with a CO_2 removal efficiency of 90%. This means a 25% energy reduction for CO_2 capture issues.

Further research lines suggest the execution of this model aiming to find an optimal solvent considering both separation degree and ecological footprint, such a solvent could be a mixture of amines or a mixture amines–ionic liquids. Additionally, the dynamic optimization of the start-up procedures for this process is an interesting topic to explore.

NOTATION

Variables

a^l,	m^2 interfacial area
a_p,	m^2/m^3 specific surface area of the packing
A_ϕ,	$\sqrt{\frac{kg}{mol}}$ Debye–Hückel parameter
c,	$kmol/m^3$ molar concentration
Cp,	kJ/(kg K) specific heat
d_eq,	m equivalent diameter
d_p,	m nominal packing size
D,	m^2/hr diffusivity
D^{crit},	m^2/hr critical diffusion coefficients for ions
D^o,	m^2/hr mutual diffusion coefficient at infinite dilution
e,	kJ/hr heat transfer rate across the film
E	enhancement factor
f,	kmol/hr feed molar rate
g,	m/hr^2 gravity constant
G,	term to local contribution
h,	kJ/kmol liquid phase enthalpy
$\hat{h}$,	kJ/kmol liquid phase partial enthalpy
H,	atm Henry coefficient
H,	kJ/kmol vapor phase enthalpy
$\hat{H}$,	kJ/kmol vapor phase partial enthalpy
H,	kJ/(m^2 hr K) heat transfer coefficient
H^{vap},	kJ/kmol enthalpy of vaporization
Ha	Hatta number
H_f,	kJ/kmol enthalpy of formation
$ionm$	ion mobility
I_x	ionic strength

J, kmol/(m^2 hr) diffusion flux
k, m/hr binary mass transfer coefficient
k_B, J/K Boltzmann constant
K phase equilibrium constant
K, m^3/(kmol hr) kinetic reaction pre-exponential factor
K_{eq} chemical equilibrium constant
L, kmol/hr liquid phase molar rate
Le Lewis number
M, kg/kmol molar mass
N, kmol/hr mass transfer rate across the film
P, atm pressure
q_e, C electron charge
r, m Born radius of the ionic species
R, kJ/(kmol K) ideal gas constant
R, hr/m reciprocal mass transfer rate matrix
Re Reynolds number
Re' Reynolds number based on interfacial area
S, m structured packing's channel side
Sc Schmidt number
Sh Sherwood number
T, K temperature
T_c, K critical temperature
T_o, K reference temperature
Tr reduced temperature
u, m/hr fluid velocity
V, kmol/hr vapor phase molar rate
V_b, cm^3/mol liquid molar volume at the normal boiling point
x liquid phase mole fraction
y vapor phase mole fraction
z ion charge number

Greek letters

α nonrandomness factor in eNRTL model
β, (V C)/J dielectric constant
γ activity coefficient
Γ thermodynamic factor
ε, kmol/hr reaction coordinate
ϵ_o, C/(V m) permittivity of free space
κ, m/hr multicomponent mass transfer coefficient
λ, kJ/(m hr K) heat conductivity
μ, cP viscosity
ν stoichiometric coefficient
ρ, kg/m^3 density
τ energy parameter in eNRTL model
Φ association factor of solvent
χ effective local mole fraction in eNRTL model
ω acentric factor
Ω diffusion collision integral

Subscripts

an anion
c total number of components
cat cation
i component
j stage
k component
mol molecular component
r reaction

Superscripts

Born Born contribution
F feed
I interphase
L liquid phase
lc local contribution
s saturation
solv solvent
P phase
PDH Pitzer–Debye–Hückel contribution
tot total
V vapor phase
∞ infinite dilution

ORCID

Luis Angel López-Bautista https://orcid.org/0000-0003-3810-3868
Antonio Flores-Tlacuahuac https://orcid.org/0000-0001-7944-0057

REFERENCES

1. Rockström J, Steffen W, Noone K, et al. Planetary boundaries: exploring the safe operating space for humanity. *Ecol Soc*. 2009;14:1-33.
2. Ramdin M, de Loos TW, Vlugt TJ. State-of-the-art of CO_2 capture with ionic liquids. *Ind Eng Chem Res*. 2012;51:8149-8177.
3. Moioli S, Pellegrini LA, Gamba S, Li B. Improved rate-based modeling of carbon dioxide absorption with aqueous monoethanolamine solution. *Front Chem Sci Eng*. 2014;8:123-131.
4. Wang M, Lawal A, Stephenson P, Sidders J, Ramshaw C. Post-combustion CO_2 capture with chemical absorption: a state-of-the-art review. *Chem Eng Res Des*. 2011;89:1609-1624.
5. United States Environmental Protection Agency. Overview of Greenhouse Gases; 2019. https://www.epa.gov/ghgemissions/overview-greenhouse-gases. Accessed April 5th, 2019.
6. Brennecke JF, Gurkan BE. Ionic liquids for CO_2 capture and emission reduction. *J Phys Chem Lett*. 2010;1:3459-3464.
7. Yu C-H, Huang C-H, Tan C-S. A review of CO_2 capture by absorption and adsorption. *Aerosol Air Qual Res*. 2012;12:745-769.
8. Taylor R, Krishna R. *Multicomponent Mass Transfer*. 2nd ed. New York, USA: John Wiley & Sons; 1993.
9. Seader JD, Henley EJ, Roper DK. *Separation Process Principles*. New York, USA: Wiley; 1998.
10. Dugas RE. Pilot Plant Study of Carbon Dioxide Capture by Aqueous Monoethanolamine [MSc thesis]. University of Texas at Austin; 2006.
11. Neveux T, Le Moullec Y, Corriou J-P, Favre E. Modeling CO_2 capture in amine solvents: prediction of performance and insights on limiting phenomena. *Ind Eng Chem Res*. 2013;52:4266-4279.
12. Kale C, Górak A, Schoenmakers H. Modelling of the reactive absorption of CO_2 using mono-ethanolamine. *Int J Greenh Gas Control*. 2013;17:294-308.

13. Mac Dowell N, Samsatli N, Shah N. Dynamic modelling and analysis of an amine-based post-combustion CO_2 capture absorption column. *Int J Greenh Gas Control*. 2013;12:247-258.
14. Hilliard MD. A Predictive Thermodynamic Model for an Aqueous Blend of Potassium Carbonate, Piperazine, and Monoethanolamine for Carbon Dioxide Capture from Flue Gas [PhD thesis]. University of Texas at Austin; 2008.
15. Zhang Y, Que H, Chen C-C. Thermodynamic modeling for CO_2 absorption in aqueous MEA solution with electrolyte NRTL model. *Fluid Phase Equilibr*. 2011;311:67-75.
16. Versteeg G, Van Dijck L, van Swaaij WPM. On the kinetics between CO_2 and alkanolamines both in aqueous and non-aqueous solutions. An overview. *Chem Eng Commun*. 1996;144:113-158.
17. Aronu UE, Gondal S, Hessen ET, et al. Solubility of CO_2 in 15, 30, 45 and 60 mass% MEA from 40 to 120 C and model representation using the extended UNIQUAC framework. *Chem Eng Sci*. 2011;66:6393-6406.
18. Zhang Y, Chen H, Chen C-C, Plaza JM, Dugas R, Rochelle GT. Rate-based process modeling study of CO_2 capture with aqueous monoethanolamine solution. *Ind Eng Chem Res*. 2009;48:9233-9246.
19. Abu-Zahra MR, Schneiders LH, Niederer JP, Feron PH, Versteeg GF. CO_2 capture from power plants: part I. a parametric study of the technical performance based on monoethanolamine. *Int J Greenh Gas Control*. 2007;1:37-46.
20. Chu F, Yang L, Du X, Yang Y. CO_2 capture using MEA (monoethanolamine) aqueous solution in coal-fired power plants: modeling and optimization of the absorbing columns. *Energy*. 2016;109:495-505.
21. Mores P, Scenna N, Mussati S. A rate based model of a packed column for CO_2 absorption using aqueous monoethanolamine solution. *Int J Greenh Gas Control*. 2012;6:21-36.
22. Mores P, Scenna N, Mussati S. CO_2 capture using monoethanolamine (MEA) aqueous solution: modeling and optimization of the solvent regeneration and CO_2 desorption process. *Energy*. 2012;45:1042-1058.
23. Baur R, Taylor R, Krishna R. Dynamic behaviour of reactive distillation columns described by a nonequilibrium stage model. *Chem Eng Sci*. 2001;56:2085-2102.
24. Henley EJ, Seader JD. *Equilibrium-Stage Separation Operations in Chemical Engineering*. New York, USA: Wiley; 1981.
25. Onda K, Takeuchi H, Okumoto Y. Mass transfer coefficients between gas and liquid phases in packed columns. *J Chem Eng Jpn*. 1968;1:56-62.
26. Bravo JL. Mass transfer in gauze packings. *Hydrocarbon Process*. 1985;64:91-95.
27. López-Bautista AO, Flores-Tlacuahuac A, Nigam K. Optimal start-up policies for a nanofluid-based solar thermal power plant. *Ind Eng Chem Res*. 2019;58:19135-19148.
28. Wang R, Liu S, Wang L, et al. Superior energy-saving splitter in monoethanolamine-based biphasic solvents for CO_2 capture from coal-fired flue gas. *Appl Energy*. 2019;242:302-310.

SUPPORTING INFORMATION

Additional supporting information may be found online in the Supporting Information section at the end of this article.

How to cite this article: López-Bautista LA, Flores-Tlacuahuac A. Optimization of the amines-CO_2 capture process by a nonequilibrium rate-based modeling approach. *AIChE J*. 2020;1–14. https://doi.org/10.1002/aic.16978